NOT FOR DISTRIBUTION JINST_001P_0207

Benchmarking of simulation codes for high intensity hydrogen ion linacs

J.-P. Carneiro

Fermi National Accelerator Laboratory
Batavia, IL, 60510, U.S.A.

E-mail: carneiro@fnal.gov

Abstract. This document presents the benchmarking of two beam dynamics simulation codes TRACK and ASTRA with application to the FNAL superconducting 8-GeV hydrogen ion linac. TRACK, developed by Argonne National Laboratory to fulfill the requirement of heavy-ion linacs, is the main tool in the design of the accelerator. ASTRA, developed by the Deutsches Elektronen-Synchrotron laboratory (Hamburg, Germany), is mainly used for the design of electron photo-injectors and we present for the first time the possibility of this code to accelerate hydrogen ions.

1. Introduction

Fermilab is developing a High Intensity Proton Source consisting in an 8 GeV superconducting H^- linac with the primary mission of increasing the intensity of the Fermilab Main Injector for the production of neutrino superbeams. Observation of CP violation, measurement of the neutrino mass-squared differences and general understanding of neutrino properties are goals of the U.S. neutrino programs this accelerator is designed to accomplish. Figure 1 presents a layout of the linac :

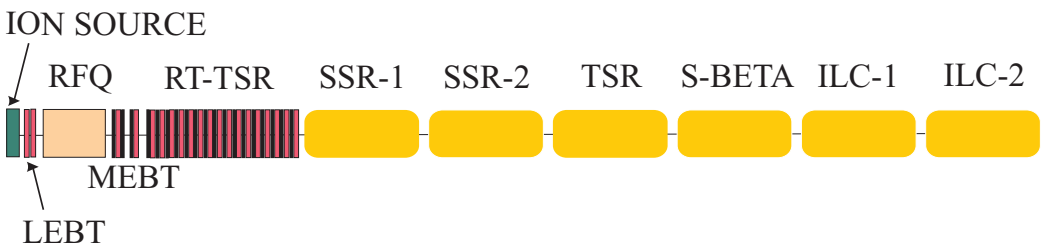

Figure 1. Layout of the Fermilab High Intensity Proton Source.

The main elements of the accelerator are an H^- Ion Source, a Low Energy Beam Transport (LEBT) to match the beam into a Radio-Frequency Quadrupole (RFQ), a Medium Energy Beam Transport (MEBT) with 2 Room Temperature (RT) bunching cavities and a beam chopper followed by 16 RT Triple Spoke Resonators (RT-TSR), 18 superconducting Single Spoke Resonators of Type 1 (SSR1) and 33 longer ones (SSR2), 42 superconducting Triple Spoke Resonators (TSR), 56 Squeezed ILC-type superconducting cavities (S-ILC) designed for $\beta_G = 0.81$ and 287 ILC-type cavities. The transverse focusing up to the TSR section is achieved with 57 superconducting solenoids and beyond with 117 normal conducting quadrupoles. The ILC-type section is divided in 9 cryomodules containing 2 quadrupoles and 7 cavities (ILC1) followed by 28 cryomodules with 1 quadrupole and 8 cavities (ILC2). The length and output kinetic energy W_{out} of each section is presented in Table 1. A detailed description of the accelerator can be found in References [1] and [2].

Table 1. Linac main section lengths and output kinetic energy.

Section	**Length**	**W_{out}**
Ion Source+LEBT	∼0.2 m	50 keV
RFQ	∼4.0 m	2.5 MeV
MEBT+RT-TSR	12.6 m	8.8 MeV
SSR1+SSR2	43.1 m	121 MeV
TSR	81.6 m	421 MeV
S-ILC	85.4 m	1.2 GeV
ILC1+ILC2	451.4 m	8 GeV

NOT FOR DISTRIBUTION JINST_001P_0207

The accelerator is designed to deliver $1.56{\cdot}10^{14}$ protons to the FNAL Main Injector in typical bunch lengths of 1 msec leading to an average beam current of 25 mA per pulse. At a beam kinetic energy of 8 GeV and a repetition rate of 10 Hz the corresponding beam average power is ∼2 MW. An outstanding feature of this accelerator is the use of ferrite phase shifters [3] which allow a small number of klystrons to power the cavities. In fact, in the baseline design, a single 325 MHz klystron is foreseen to power the front-end linac (from IS to TSR section), and 10 ILC-type klystrons operating at 1300 MHz are required for the remaining section of the accelerator.

2. Code description

2.1. Integration of the equations of motion

The general equations of motion for a particle in an electromagnetic field are :

$$\frac{d\vec{r}}{dt} = \frac{\vec{p}}{m_0\gamma} \tag{1}$$

$$\frac{d\vec{p}}{dt} = q(\vec{E} + \frac{\vec{p}}{m_0\gamma} \times \vec{B}) \tag{2}$$

with $\vec{r}$ the particle coordinate, $\vec{p}$ the mechanical momentum, $\gamma = \sqrt{1-\beta^2}$, $\beta = v/c$, v and c particle and light speed, q and m_0 charge and rest mass of accelerated particle and $\vec{E}$ and $\vec{B}$ the electric and magnetic fields. Both codes `TRACK` [4] and `ASTRA` [5] perform the integration of Equations (1) and (2) by the Runge-Kutta method of forth order, with a variable integration step size for both codes. `TRACK` uses a spatial integration step defined for each element of the beam line while `ASTRA` uses a user defined temporal integration step. The fields $\vec{E}$ and $\vec{B}$ include external contribution from accelerating and focusing fields and internal from the beam space charge forces. Both codes have the ability of using 2D external electric fields defined on the cavity axis or 3D external electric fields defined on a rectangular mesh. Concerning the external solenoid magnetic fields, `TRACK` can handle both 2D or 3D fields while `ASTRA` does support only 2D ones. For the simulations presented in this document, both codes were provided with the exact 3D electric fields, in binary format for `TRACK` and ASCII for `ASTRA`, and with the exact 2D solenoid magnetic fields on axis in ASCII format. `TRACK` and `ASTRA` performs then the same polynomial expansion to 3^{rd} order as :

$$B_z(z,r) = B_z(z,0) - \frac{r^2}{4}\left(\frac{d^2B}{dz^2} - \frac{d^4B}{dz^4}\frac{r^2}{16} + \frac{d^6B}{dz^6}\frac{r^4}{576}\right) \tag{3}$$

$$B_r(z,r) = -\frac{r}{2}\left(\frac{dB}{dz} - \frac{d^3B}{dz^3}\frac{r^2}{8} + \frac{d^5B}{dz^5}\frac{r^4}{192}\right) \tag{4}$$

with $B_{z,0}$ the longitudinal on-axis magnetic field.

NOT FOR DISTRIBUTION JINST_001P_0207

For the simulations presented in this paper, the space-charge forces were computed using the 3D space charge calculation available in TRACK and ASTRA. For both codes, the space-charge fields are calculated in the beam rest frame via Poisson's equation :

$$\nabla^2\phi(r,\theta,z) = -\frac{\rho(r,\theta,z)}{\epsilon_0} \tag{5}$$

with ϕ the electrostatic potential, ρ the charge density, ϵ_0 the dielectric constant and Lorentz's transformed back into the laboratory frame. A 3D Cartesian grid is used for both codes with the calculation of the electrostatic potential at each grid points. On the boundaries, TRACK considers ideal parallel conducting walls transversely and free-space longitudinally while ASTRA solves the Poisson's equation in free-space.

Finally, it is important to notice that, unlike TRACK, the code ASTRA does not handle RFQ's. Therefore, the codes benchmarking does start at the exit of this element.

2.2. Output parameters

TRACK and ASTRA provide several beam output parameters and, for TRACK, some parameters are output in several units. In this document we consider the following ones: RMS transverse size σ_x and σ_y, RMS normalized transverse emittance ϵ_x and ϵ_y, RMS bunch length σ_z, RMS normalized longitudinal emittance ϵ_z, kinetic energy W and RMS energy spread σ_E. The ASTRA units for these parameters are taken as reference and are depicted in the following. The RMS normalized transverse emittance is defined in this document by the relation :

$$\epsilon_u = \beta\gamma\sqrt{\langle u^2\rangle\langle (u')^2\rangle - \langle uu'\rangle^2}; \tag{6}$$

with m_0 and c the parameters defined in the previous section, u and u' the transverse coordinate and divergence of x or y, and $\langle\rangle$ an RMS value.

3. Methodology

Benchmarking of TRACK and ASTRA is presented in this document from the exit of the RFQ up to the last accelerating section (ILC2), which represents a length of ∼674 m. First the Zero Current case is considered for its simplicity. In fact, in this scenario, the benchmarking does not take into account the space charge effects implying linear beam dynamics and fast simulations. Then the benchmarking is realized for a linac peak current of 43.25 mA. Indeed, Reference [2] mentions that in order to avoid beam losses during RF capture and to provide a gap for the extraction kicker in the Main Injector, a linac peak current of 43.25 mA is necessary to deliver the desired 25 mA peak current to the Main Injector.

Beam dynamics simulation in the RFQ has been performed with TRACK as presented in Reference [6] providing, at the RFQ exit, two particle distribution of $1{\cdot}10^3$ and $2{\cdot}10^5$ particles for respectively the Zero Current and the 43.25 mA cases. Table 2 shows the beam parameters of each initial distribution as provided to TRACK and ASTRA.

NOT FOR DISTRIBUTION JINST_001P_0207

NOT FOR DISTRIBUTION JINST_001P_0207

Table 2. Initial beam parameters (at $z = 0$ m, RFQ exit).

Beam parameters	**Zero Current**	**43.25 mA**
RMS size σ_X	0.69 mm	0.74 mm
RMS size σ_Y	0.68 mm	0.72 mm
Norm. RMS emittance ϵ_X	0.25 mm-mrad	0.25 mm-mrad
Norm. RMS emittance ϵ_Y	0.26 mm-mrad	0.25 mm-mrad
RMS bunch length σ_Z	1.75 mm	1.85 mm
Norm. RMS emittance ϵ_Z	45.9 kev-mm	25.6 kev-mm
Kinetic Energy W	2.51 MeV	2.52 MeV
RMS energy spread σ_E	28.6 keV	17.8 keV

4. Code Benchmarking

4.1. Zero Current

Figure 2 presents `TRACK` and `ASTRA` simulations of the High Intensity Proton Source, from the RFQ exit to the last ILC2 cryomodule for Zero Current. The final beam parameters of both codes are presented in Table 3.

Table 3. `TRACK` and `ASTRA` outputs for Zero Current (at $z \simeq 674$ m).

Beam parameters	**TRACK**	**ASTRA**
RMS size σ_X	1.71 mm	1.88 mm
RMS size σ_Y	0.98 mm	0.97 mm
Norm. RMS emit. ϵ_X	0.263 mm-mrad	0.265 mm-mrad
Norm. RMS emit. ϵ_Y	0.258 mm-mrad	0.260 mm-mrad
RMS bunch length σ_Z	0.251 mm	0.256 mm
Norm. RMS emit. ϵ_Z	643 kev-mm	648.2 kev-mm
Kinetic Energy W	7971 MeV	7973 MeV
RMS energy spread σ_E	2630 keV	2565 keV

An overall excellent agreement between the simulation codes `TRACK` and `ASTRA` is presented in Figure 2 and Table 3 for the Zero Current case. The longitudinal parameters (RMS bunch length, RMS normalized longitudinal emittance, kinetic energy and RMS energy spread) are within 3% between the simulation codes at the end of the linac, after ∼674 meters of simulations. Concerning the transverse parameters, the RMS size of the beam differs between both codes, by ∼10% horizontally and by ∼1% vertically. Also a slight difference in the RMS transverse emittance between `TRACK` and `ASTRA` can be observed in Figure 2(b), the transverse emittance from `ASTRA` being slightly higher (∼0.7% horizontally and vertically) than the one from `TRACK`. A possible explanation for this difference is the different step size used by the simulation codes for the integration of the equations of motion (1) and (2) by the Runge-Kunta method of fourth order.

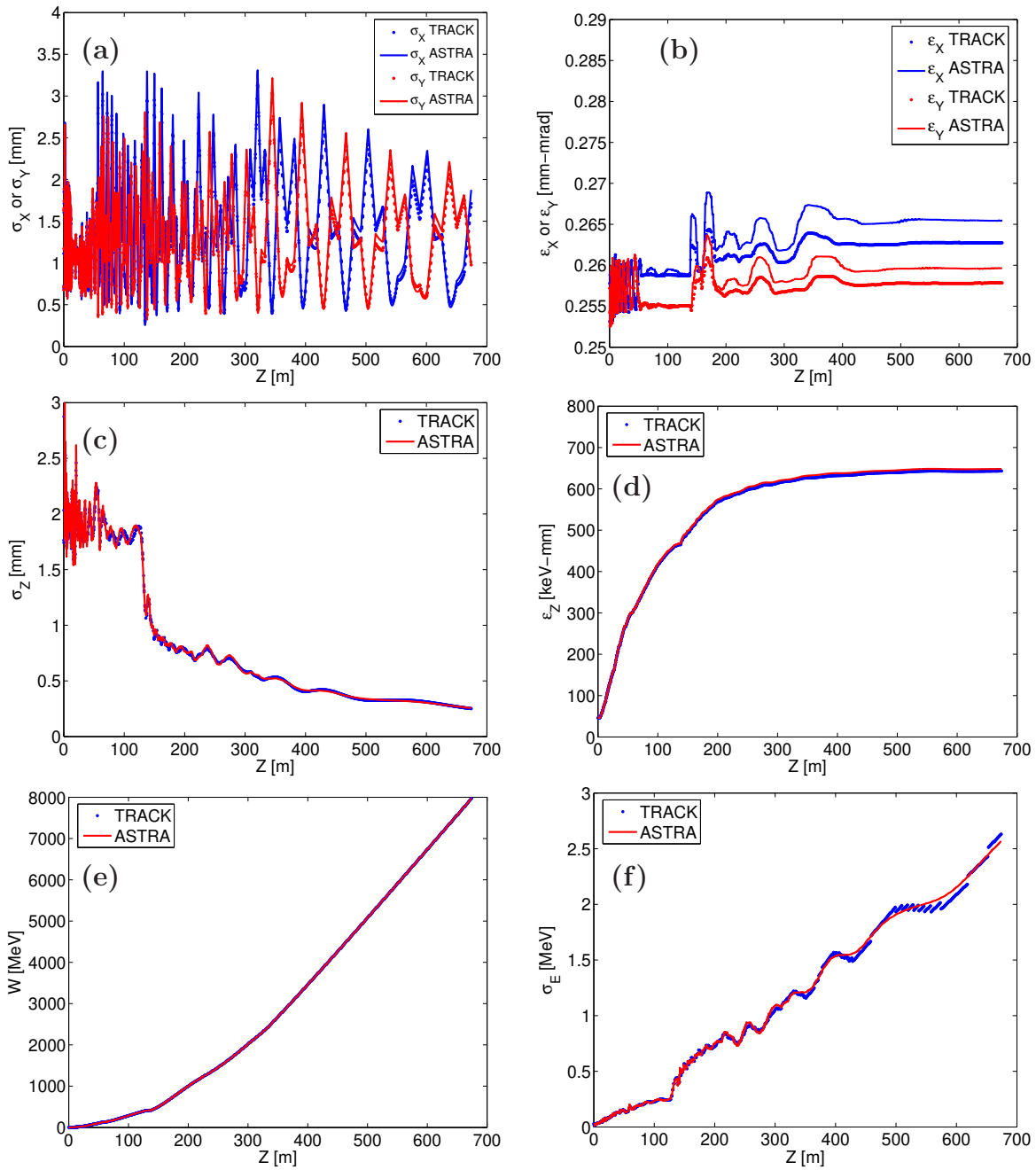

Figure 2. TRACK and ASTRA simulations of the High-Intensity Proton Source with Zero Current, from the RFQ exit ($z = 0$ m) to the last accelerating cavity ($z \simeq 674$ m) . From top left to bottom right: (a) RMS transverse size, (b) RMS normalized transverse emittance, (c) RMS bunch length, (d) RMS normalized longitudinal emittance, (e) kinetic energy and (f) RMS energy spread.

The impact of the integration step size on the beam dynamics simulations is presented in Figure 3 with ASTRA simulations of the RMS transverse size and RMS normalized transverse emittance for the ILC1+ILC2 section (total length of ∼451.4 meters, see Table 1) of the High Intensity Proton Source at Zero Current using four

NOT FOR DISTRIBUTION JINST_001P_0207

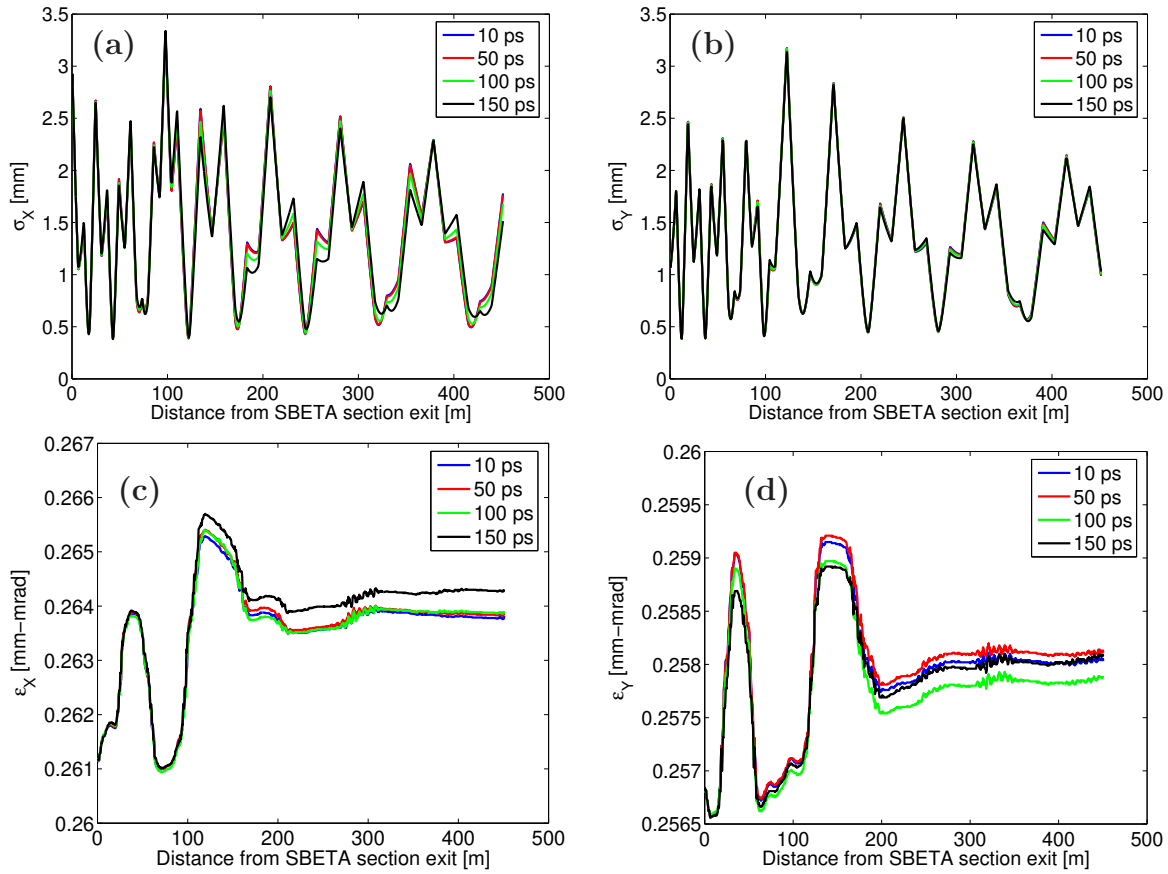

Figure 3. ASTRA simulations of the ILC1+ILC2 section of the High Intensity Proton Source (total length ∼451.4 m), at Zero Current and four different integration time steps: 10 ps, 50 ps, 100 ps and 150 ps.

different integration time steps: 10 ps, 50 ps, 100 ps and 150 ps. This figure confirms that the accuracy of the simulations depends on the integration step size, the smaller the time step the higher the accuracy.

Defining the same integration step size for both code is not realistic, since TRACK uses a spatial step size defined for each beam line element while ASTRA uses a temporal step which was defined at Zero Current between 60 ps and 150 ps as a trade-off between accuracy and CPU time. Therefore, this difference in the integration step size between the code will ineluctably lead to a discrepancy between the output parameters, as presented in Table 3.

4.2. 3D Uniform Ellipsoidal Bunch

As an intermediate step towards the code benchmarking at high peak current, the transverse and longitudinal on-axis space charge fields of an ideal 3D uniform ellipsoidal bunch was calculated by the 3D space routine of TRACK and ASTRA and compared with the analytical expressions. In fact, 3D uniform ellipsoidal distributions represent the only distribution whose space charge field can be calculated analytically. Inside the

NOT FOR DISTRIBUTION JINST_001P_0207

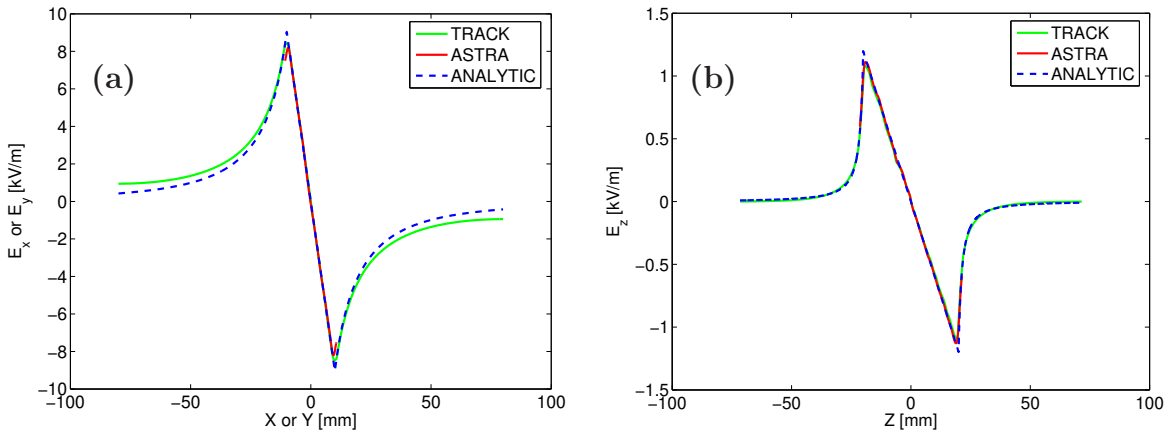

Figure 4. (a) Transverse and (b) Longitudinal electric field of an uniform ellipsoidal bunch from `TRACK`, `ASTRA` and analytical method.

ellipsoid the space-charge fields are a linear function of the position and can be expressed in the bunch rest by [7]:

$$E_x^{sc} = \frac{I\lambda(1-f)}{4\pi\epsilon_0 c(r_x+r_y)r_z}\cdot\frac{x}{r_x} \qquad x \le r_x \tag{7}$$

$$E_y^{sc} = \frac{I\lambda(1-f)}{4\pi\epsilon_0 c(r_x+r_y)r_z}\cdot\frac{y}{r_y} \qquad y \le r_y \tag{8}$$

$$E_z^{sc} = \frac{I\lambda f}{4\pi\epsilon_0 c r_x r_y}\cdot\frac{z}{r_z} \qquad z \le r_z \tag{9}$$

with I the average current over an RF period, λ the RF wavelength, f a geometrical form factor, ϵ_0 the permittivity of free space, r_x, r_y and r_z the semi-axes of the ellipse in the laboratory frame which are related to the RMS beams sizes σ_x, σ_y and σ_z by $r_x = \sqrt{5}\cdot\sigma_x$, $r_y = \sqrt{5}\cdot\sigma_y$ and $r_z = \sqrt{5}\cdot\sigma_z$.

For ellipsoidal distributions of equal transverse sizes ($r_x = r_y$) the form factor f depends on the parameter $p = \gamma r_z/\sqrt{r_x r_y}$ with γ the Lorentz factor and satisfies [8]:

$$f = \int_0^1 \frac{\nu^2 d\nu}{\left[p^2+(1-p^2)\nu^2\right]^2} \tag{10}$$

The space charge fields outside the ellipsoid are given also by Equations (7)-(9) with $r_x = \sqrt{r_x^2+\chi}$, $r_y = \sqrt{r_y^2+\chi}$ and $r_z = \sqrt{r_z^2+\chi}$ where the external point (x,y,z) verifies the Equation :

$$\frac{x^2}{r_x^2+\chi} + \frac{y^2}{r_y^2+\chi} + \frac{z^2}{r_z^2+\chi} = 1 \tag{11}$$

Figure 4 shows the comparison between the analytical space charge fields on the transverse and longitudinal axis of a 3D uniform ellipsoid filled with $2{\cdot}10^5$ particles of unit charge (with semi-axis length of 1 cm transversely and 2 cm longitudinally) and the simulation codes `TRACK` and `ASTRA`. On the longitudinal axis, the agreement is excellent.

NOT FOR DISTRIBUTION JINST_001P_0207

On the transverse axis, the space charge field provided by TRACK outside the bunch slightly differs from the one computed from the analytical expressions. As mentioned in Section 2.1, TRACK computes the space charge fields taking into account the image charge of the beam on the conducting wall surface. Reference [9] mentions that the image charge increases the radial defocussing space charge fields, which explains the difference observed in Figure 4(a). At the conditions of using a sufficiently high number of macro-particles and properly setting up the space charge grids, TRACK and ASTRA provide similar space charge fields for similar input distributions.

4.3. 43.25 mA

Figure 5 present TRACK and ASTRA simulations of the High Intensity Proton Source, from the RFQ exit to the last ILC2 cyomodule for a linac peak current of 43.25 mA. The final beam parameters of both codes are presented in Table 4.

Table 4. TRACK and ASTRA outputs for 43.25 mA (at $z \simeq 674$ m).

Beam parameters	**TRACK**	**ASTRA**
RMS size σ_X	1.76 mm	1.87 mm
RMS size σ_Y	1.32 mm	1.31 mm
Norm. RMS emit. ϵ_X	0.458 mm-mrad	0.505 mm-mrad
Norm. RMS emit. ϵ_Y	0.549 mm-mrad	0.557 mm-mrad
RMS bunch length σ_Z	0.345 mm	0.351 mm
Norm. RMS emit. ϵ_Z	857 kev-mm	1175.1 kev-mm
Kinetic Energy W	8013 MeV	8022 MeV
RMS energy spread σ_E	2564 keV	3397 keV

For space charge calculations, a grid of 64×64×64 was implemented into ASTRA and an adjustable grid of 65×65×129 for the first two cavities, 65×65×65 in the SC Single-Spoke Resonator section and 129×129×65 beyond into TRACK. Figure 5 and Table 4 report that the transverse beam dynamics agrees within 10% between both codes and, as previously mentioned, integration steps might explain this disagreement. In contrast to the zero current case, some disagreement concerning longitudinal beam dynamics is observed starting from the S-ILC section (∼137 m). The longitudinal disagreement is more pronounced for the longitudinal emittance and energy spread than the bunch length but stays within ∼10% between both codes. Figure 6 presents the longitudinal phase space from TRACK and ASTRA at $z \simeq 674$ m and confirms the good agreement between both simulation codes.

5. Conclusion

A benchmarking of the simulation codes TRACK and ASTRA has been presented in this paper with an application to the FNAL superconducting H^- linac. The simulations were

NOT FOR DISTRIBUTION JINST_001P_0207

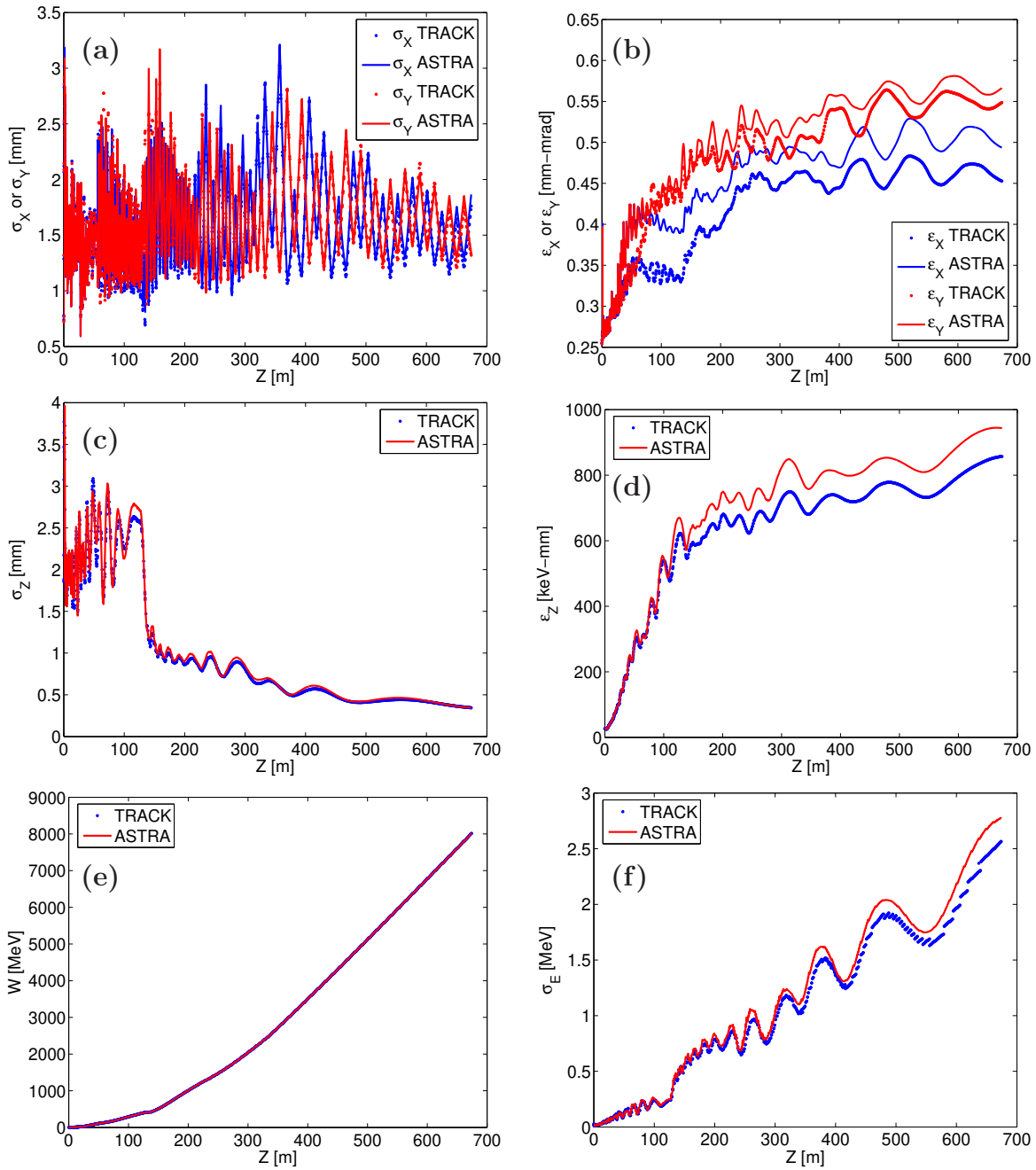

Figure 5. `TRACK` and `ASTRA` simulations of the High-Intensity Proton Source for a linac peak current of 43.25 mA, from the RFQ exit ($z = 0$ m) to the last accelerating cavity ($z \simeq 674$ m). From top left to bottom right: (a) RMS transverse size, (b) RMS normalized transverse emittance, (c) RMS bunch length, (d) RMS normalized longitudinal emittance, (e) kinetic energy and (f) RMS energy spread.

performed on an overal length of ∼674 meters (including 454 cavities, 117 quadrupoles and 55 solenoids), with an energy ranging from ∼2.5 MeV to ∼8 GeV and for two operating currents: Zero Current (space charge off) and 43.25 mA peak (using 3D space charge routine). A good agreement (within 10%) was found between both codes for

NOT FOR DISTRIBUTION JINST_001P_0207

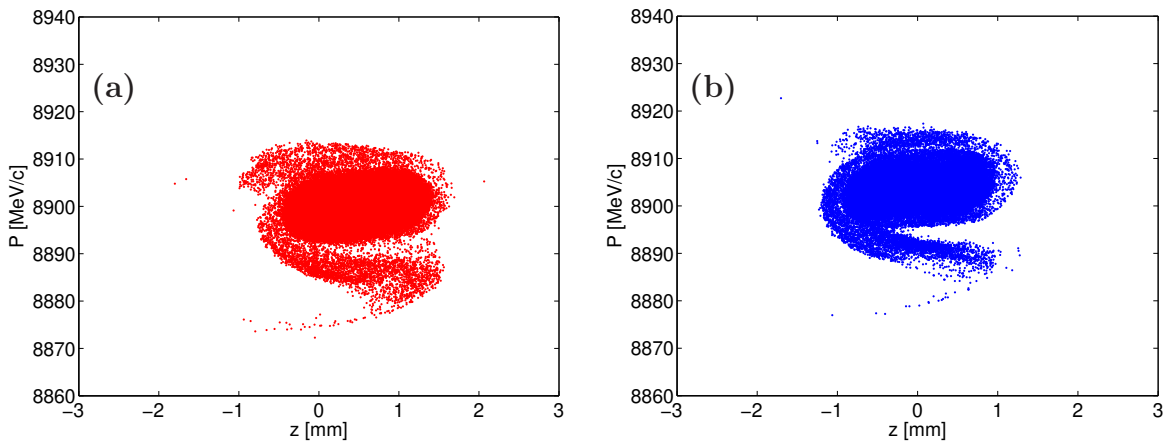

Figure 6. (a) TRACK and (b) ASTRA longitudinal phase space at the last accelerating cavity ($z \simeq 674$ m) of the High-Intensity Proton Source for a linac peak current of 43.25 mA.

the transverse and longitudinal parameters. An earlier version of this paper has been presented in Reference [10].

Acknowledgments

The author would like to thank P. Ostroumov and V. Aseev (ANL) for helpful discussions about TRACK, K. Flöttmann (DESY) for his support in using ASTRA, B. Webber and V. Shiltsev (FNAL) for their encouragement.

References

[1] G.W. Foster (Editor), *An 8-GeV Superconducting Linac Proton Driver*, available at : http://protondriver.fnal.gov/SCRF_PD_v56.doc

[2] P.N. Ostroumov, *Physics design of the 8-GeV H-minus Linac* , New Journal of Physics, **8**, 281 (2006).

[3] R. Madrak et al.,*New Materials and Designs for High-Power, Fast, Phase Shifters*, Proceedings of Linear Accelerator Conference, Knoxville, Tennessee (2006).

[4] V.N. Aseev, P.N. Ostroumov, E.S. Lessner and B. Mustapha, *TRACK : The new beam dynamics code*, Proceedings of Particle Accelerator Conference, Knoxville, Tennessee (2005).

[5] K. Flöttmann, ASTRA user manual available at : http://www.desy.de/ ˜mpyflo/Astra_dokumentation/

[6] P.N. Ostroumov, V.N. Aseev and A.A. Kolomiets, *Application of a new procedure for design of 325 MHz RFQ*, Journal of Instrumentation, **1**, P04002 (2006).

[7] T. Wangler, *RF Linear Accelerators*, John Wiley &. Sons, Inc., pp. 277, equation 9.40 (1998).

[8] M. Comunian et al., *Frequency map analysis of a three-dimensional particle in the core of a high intensity linac*, Physical Review Special Topics-Accelerator and beams, Vol. **4**, 124201, (2001).

[9] M. Reiser, *Theory and Design of Charged Particle Beams*, Wiley-Interscience, pp. 406 (1994).

[10] J.-P. Carneiro, *Benchmarking of Simulation Codes TRACK (ANL) and ASTRA (DESY) for the FNAL High-Intensity Proton Source*, Proceedings of Linear Accelerator Conference, Knoxville, Tennessee (2006).

NOT FOR DISTRIBUTION JINST_001P_0207